Available online at www.sciencedirect.com
ScienceDirect
International Journal of Thermal Sciences 46 (2007) 649–661
International Journal of Thermal Sciences
www.elsevier.com/locate/ijts

Inverse radiation analysis of a one-dimensional participating slab by stochastic particle swarm optimizer algorithm

H. Qi, L.M. Ruan *, H.C. Zhang, Y.M. Wang, H.P. Tan

School of Energy Science and Engineering, Harbin Institute of Technology, 92, West Dazhi street, Harbin 150001, PR China

Received 4 October 2005; received in revised form 4 October 2006; accepted 4 October 2006

Available online 13 November 2006

Abstract

A stochastic particle swarm optimizer (SPSO) algorithm, which can guarantee the convergence of the global optimization solution with probability one, is adopted to estimate the parameters of radiation system. To illustrate the performance of this algorithm, three cases are investigated, in which the source term, the extinction coefficient, the scattering coefficient, and the non-uniform absorption coefficients in a one-dimensional slab are retrieved. The directional radiative intensity, reflectance and transmittance, radiative flux simulated by discrete ordinate method (DOM) are served as input for the inverse analysis, respectively. By SPSO algorithm presented, all these radiative parameters could be estimated accurately, even with noisy data. In conclusion, the SPSO algorithm is proved to be fast and robust, which has the potential to be implemented in various fields of inverse radiation problem.

Keywords: Inverse radiation analysis; Stochastic particle swarm optimizer algorithm; Discrete ordinate method

1. Introduction

Inverse radiation analysis is concerned with the determination of the radiation properties, boundary condition, and the temperature profile or source term distribution from various types of radiation measurements, which is very practical and useful in many different areas, e.g., laser light-scattering flame diagnose, optical tomography in medical imaging, remote sensing of the atmosphere, the prediction of the temperature distribution in combustion chambers, and optimizing the manufacturing and materials processing system. An extensive review of the early development has been given in a series of papers by McCormic [1,2]. Recently, a number of papers has examined various inverse radiation problems on determining the single-scattering albedo, scattering phase function, absorption coefficient, scattering coefficient, boundary condition, or the optical thickness of a medium from various types of radiation measurements [3–8]. Meanwhile, a wide variety of solution techniques has been successfully employed in these inverse radiation analyses such as the conjugate gradient (CG) method [9], and Levenberg–Marquardt method [10]. However, all these traditional methods depend on the initial value or the derivatives and gradients which are difficult to be solved accurately by numerical simulation in some cases. Furthermore, if the initial value is not chosen properly, the solution may be infeasible in the original domain, or in a worse case, not be convergent. In a word, the traditional algorithms based on gradient method can only provide a local optimum solution depending on the initial value [11]. In order to solve the global optimal problem reliably, many researchers turned to study the random optimal method with less dependence on the objective function's analytic character. More recently, heuristic algorithms such as Genetic Algorithm (GA) and evolutionary computation have been proposed for solving the inverse radiation problems [12]. Their results were promising and encouraging for further research. Unfortunately, some deficiencies have been identified in GA performance through recent survey [13]: the degradation in efficiency is apparent in applications with highly epistatic objective functions, i.e. where the parameters being optimized are highly correlated; meanwhile, the premature convergence of GA also degrades its performance and reduces its search capability. Hence, it greatly needs to seek a more general method

* Corresponding author. Fax: (+86) 0451 6221048.
E-mail address: ruanlm@hit.edu.cn (L.M. Ruan).

1290-0729/$ – see front matter
doi:10.1016/j.ijthermalsci.2006.10.002

Nomenclature

a_n	the source term coefficients
c_1, c_2	the two positive acceleration coefficients in Eq. (1)
F	objective function of minimization
g	the scattering asymmetry parameter
M	the number of particles in each swarm
N	the maximum number of generation
n	the dimension of the problem
$\mathbf{P}_g(t)$	the global best position discovered by all particles at generation t
$\mathbf{P}_i(t)$	the local best position of particle i discovered at generation t or earlier
q	the normal incident flux
$\mathbf{q}$	the array of radiative flux
r_1, r_2	uniform random number in [0, 1]
$S(\tau)$	the function of source term ..... $\mathrm{W\,m^{-2}}$
$x_{ij}(t)$	the position of the ith particle with jth dimension at generation t ($i = 1, \ldots, M$; $j = 1, \ldots, n$)
x	x-axis coordinates
$\mathbf{X}_i(t)$	the position array of the ith particle at generation t
$v_{ij}(t)$	the velocity of the ith particle with jth dimension at generation t ($i = 1, \ldots, M$; $j = 1, \ldots, n$)
$\mathbf{V}_i(t)$	the velocity array of particles at generation t
Y	measured or exact parameter
δ	measured errors of radiative parameters
ε	a small specified positive number
ς	random variable
σ	standard deviation
Φ	scattering phase function
ω	single scattering albedo
Ω	solid angle ..... sr
τ	optical thickness
κ_a	absorption coefficient ..... $\mathrm{m^{-1}}$
κ_e	extinction coefficient ..... $\mathrm{m^{-1}}$
κ_s	scattering coefficient ..... $\mathrm{m^{-1}}$

Subscripts

av	average value
b	blackbody
est	estimated value
k	kth iteration
L_2	L_2-type norm
m	the direction of discrete ordinate
mea	measured value
min	the minimum value
max	the maximum value
R	reflectance
rel	relative value
T	transmittance

Superscripts

T	the transposed array

to solve the inverse radiative problem at arbitrary space. Unlike GA and traditional methods, the Particle Swarm Optimization (PSO) algorithm is able to find a global optimum solution or a good approximation of the solution, usually without a theoretical proof [14]. This is solely due to its ability to explore the search domain with 'jump' from a local solution to another and therefore, the global optimum solution can be reached step by step. As reported in Ref. [15], many kinds of problems which can be solved by GA are able to be identically solved by PSO, without suffering from the difficulties of GA's.

PSO algorithm, first introduced in 1995 by Eberhart and Kennedy [16], has been studied extensively by many researchers in recent years. It was originally inspired by social behavior simulation motivated by observations of the flocking behavior of birds. As a searching method, it combines the concept of survival-of-the-fittest among string patterns with a regulated yet randomized information exchange. Generally speaking, PSO is characterized to be simple in concept, easy to implement, and computationally efficient. Unlike other heuristic techniques, PSO has a flexible and well-balanced mechanism to enhance the global and local exploration abilities. The basic PSO algorithm comprises a very simple concept and its paradigms can be implemented in a few lines of computer code. It requires only primitive mathematical operators and is computationally inexpensive in terms of both memory requirements and CPU time. Another feature of PSO is the use of the objective function instead of using derivatives (sensitivity analysis) or other auxiliary knowledge. Consequently, it is not restricted to the conditions of continuity, sensitivity, convexity, monotonicity and non-linearity of both objective functions and constraints. Early studies have found the implementation of PSO to be effective and robust in solving problems featuring non-linearly, non-differentiability and high dimensionality. Many modifications have been made to improve the convergence rate of the original PSO algorithm and to increase the diversity of particles, for example, introducing the inertia weight to balance global and local search, using an adaptive fuzzy weight controller to optimize the inertia weight dynamically, using a constriction factor to improve convergence, using selection to determine the best particle, using the sequential niche technique to find multiple global optima of a function. Nowadays PSO has gained much attention and wide applications, including artificial neural network weights system [16], generation expansion planning (GEP) problem [17], discrete combinatorial optimization of polygonal approximation problems [18], and task assignment problem [19].

However, to the author's best knowledge, there were few reports concerning the application of PSO to inverse radiation analysis. In view of its practical applications to inverse radiation analysis, the advantages can be summarized as follows: Firstly, there are few parameters that PSO requires tuning, so we can just employ the experiential settings to ensure convergence in various inverse radiation analyses at arbitrary space. Secondly, in that PSO requires only primitive mathematical op-

erators, without derivative operators or genetic operators such as reproduction, crossover and mutation, the whole calculation procedure of PSO is relatively simple and easy to be implemented. Thirdly, the objective function is directly used as fitness function to guide the search in PSO, so it is easy to handle non-linear and non-differentiate inverse radiation problem. Finally, using discrete numbers for particle's position and velocity, PSO can be applied to multi-parameters and multi-peak value combinational inverse radiative problems.

In this paper, the feasibility of applying the PSO-based algorithm to radiative inverse analysis is investigated. A novel SPSO algorithm, based on stochastic particle swarm optimizer, is proposed to solve the objective function. Compared with the standard PSO algorithm, SPSO is proved to be more efficient and robust. This approach is applied to solve the inverse problem for retrieving the source term coefficients, the extinction coefficient and the scattering coefficient, and the non-uniform absorbing coefficients in a one-dimensional slab. The remainder of this paper is organized as follows: The basic PSO and its variants are described in Section 2. The detailed computation procedures of PSO and SPSO algorithm are presented in Section 3, respectively. After verifying the effective performance of SPSO compared with PSO in Section 4, SPSO algorithm is used to estimate the extinction coefficient and scattering coefficient, the spatially varying absorbing coefficients in Section 5. The effects of measurement errors on the estimation accuracy are also examined in Section 5. In Section 6, the main conclusions and perspectives are provided.

2. Theoretical overview of PSO and SPSO

The PSO algorithm is an adaptive and robust parameter searching technique based on the conceptual model of bird foraging. It is indeed a population-based stochastic algorithm which belongs to the evolutionary computation (EC) techniques. The main difference between the PSO and EC algorithms is that the PSO algorithm stores information about both its position and its velocity (change in position). However, the PSO finds the optimum value more quickly than traditional evolutionary algorithm. It is due to the fact that PSO uses a combination of local and global searches with the sharing evolutionary information among the individual particles. In this section, the basic PSO and its variants are described first, and then a modified PSO with a stochastic selection is investigated.

2.1. Basic PSO algorithm

The basic idea of PSO can be described in an explicit way: each individual in particle swarm, referred to as a 'particle', represents a potential solution; each particle moves its position in search domain and updates its velocity according to its own flying experience and neighbor's flying experience, aiming at a better position for itself as illustrated in Fig. 1. The basic elements of PSO technique are briefly stated and defined as follows:

Particle $\mathbf{X}(t)$: It is a candidate solution represented by an n-dimensional vector, where n is the number of optimization variables. At generation t, the ith particle $\mathbf{X}_i(t)$ can be described as $\mathbf{X}_i(t) = [x_{i1}(t), x_{i2}(t), \ldots, x_{in}(t)]^{\mathrm{T}}$, where $x_{ij}(t)$ is the position of the ith particle with respect to the jth dimension, i.e. the value of the jth optimized parameter in the ith candidate solution.

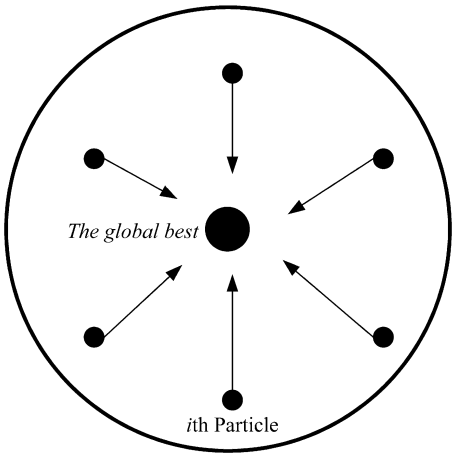

Fig. 1. Interaction between particles and the global best particle in PSO.

Swarm: It is an apparently disorganized population of moving particles that tend to cluster together while each particle seems to be moving in a random direction.

Particle velocity $\mathbf{V}(t)$: It is the velocity of the moving particles, which is represented by an n-dimensional vector. At generation t, the ith particle velocity $\mathbf{V}_i(t)$ can be described as $\mathbf{V}_i(t) = [v_{i1}(t), v_{i2}(t), \ldots, v_{in}(t)]^{\mathrm{T}}$, where $v_{ij}(t)$ is the velocity component of the ith particle with respect to the jth dimension.

Individual best position $\mathbf{P}(t)$: As a particle moves through the search space, it compares the fitness value at the current position to the best fitness value it has ever attained at any time up to the current time. The best position that is associated with the best fitness encountered so far is called the individual best position $\mathbf{P}(t)$. For each particle in the swarm, $\mathbf{P}(t)$ can be determined and updated during the searching procedure. In a minimization problem with objective function, the individual best of the ith particle $\mathbf{P}_i(t)$ is determined as $F[\mathbf{P}_i(t)] \leqslant F[\mathbf{X}_i(t')]$, $t' < t$. For the ith particle, individual best position can be expressed as $\mathbf{P}_i(t) = [p_{i1}(t), p_{i2}(t), \ldots, p_{in}(t)]^{\mathrm{T}}$.

Global best position $\mathbf{P}_g(t)$: It is the best position among all individual best positions achieved so far. Hence the global best position can be determined such that $F[\mathbf{P}_g(t)] \leqslant F[\mathbf{P}_i(t)]$, $i = 1, \ldots, M$. For the particle swarm at generation t, the global best position can be expressed as $\mathbf{P}_g(t) = [p_{g1}(t), p_{g2}(t), \ldots, p_{gn}(t)]^{\mathrm{T}}$.

The simple PSO procedure can be summarized as follows:

(1) Initialize the population, and randomly assign each particle's position and velocity. Set the initial values for local individual best location $\mathbf{P}_i$ components equal to $\mathbf{X}_i$. Pick the particle with the global optimum fitness and set it to the initial global best location $\mathbf{P}_g$. The following equation updates the velocity $\mathbf{V}_i$ for each dimension of the ith particle:

$$\mathbf{V}_i(t+1) = \mathbf{V}_i(t) + c_1 \cdot r_1 \cdot \left[\mathbf{P}_i(t) - \mathbf{X}_i(t)\right] + c_2 \cdot r_2 \cdot \left[\mathbf{P}_g(t) - \mathbf{X}_i(t)\right] \quad (1)$$

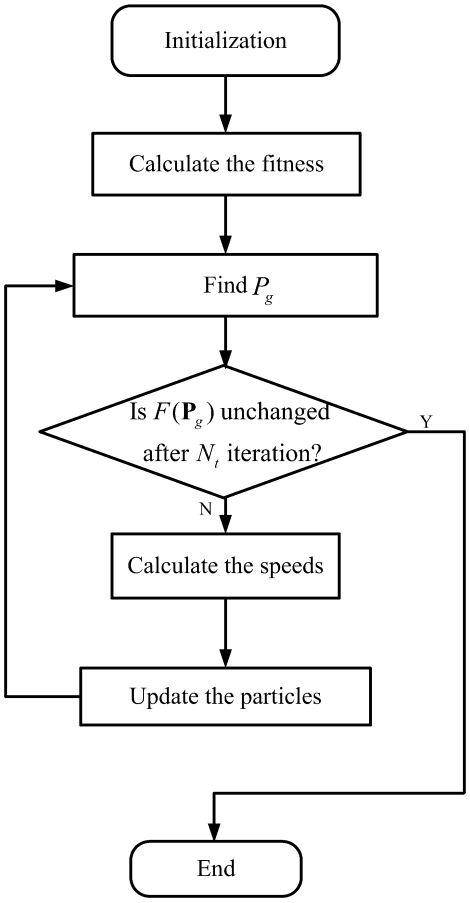

Fig. 2. The flowchart of the PSO algorithm.

where c_1 and c_2 are two positive constants called acceleration coefficients. They represent the weighting of the stochastic acceleration terms that pull each particle toward the individual best position and the overall best position, and affect the maximum size step for each particle taking in a single iteration. The new position of ith particle is expressed as:

$$\mathbf{X}_i(t+1) = \mathbf{X}_i(t) + \mathbf{V}_i(t+1) \tag{2}$$

Each position component is bounded by the maximum and minimum position component values to which each particle in the space is constrained. For the problems considered in this study, we assume that each position component is restricted to the range of $[x_{\min}, x_{\max}]$. The range of particle position is determined by the real physical meaning of the unknown parameter, e.g., the single scattering albedo of radiative medium can only be set in the range of $[0, 1]$, and the extinction coefficients of real materials must be positive and cannot be too large. In order to reduce the particle's probability of leaving the searching domain during evolution, each velocity component magnitude is usually bounded by the predetermined maximum value $v_{\max}$.

(2) Repeatedly calculate (in parallel) the new velocity and position for all particles, using Eqs. (1) and (2), and updating $\mathbf{P}_g$ and $\mathbf{P}_i$ components, until the number of cycles reaches a user-defined limit, or the non-improvement of the best solution after a given number of iterations is obtained. The flowchart of the original PSO algorithm is shown in Fig. 2.

2.2. Variants of PSO

Many modifications have been made to improve convergence speed of the original PSO algorithm and to increase the diversity of particles. Here, some usually modified PSO techniques are described briefly and more details of these modified techniques can be found in the available literatures we suggested.

2.2.1. Standard PSO with inertia weights

The flowchart in Fig. 2 was the first version of PSO proposed by Kennedy and Eberhart [16] called simple PSO model. Its main problem is that, in some occasions, the velocities tend to be infinity unless they are limited to a problem-dependent threshold. In order to improve the convergence of simple PSO, Shi and Eberhart [20] introduced an inertia weight coefficient w into this model, which can be expressed as follows:

$$\mathbf{V}_i(t+1) = w \cdot \mathbf{V}_i(t) + c_1 \cdot r_1 \cdot \left[\mathbf{P}_i(t) - \mathbf{X}_i(t)\right] + c_2 \cdot r_2 \cdot \left[\mathbf{P}_g(t) - \mathbf{X}_i(t)\right] \tag{3}$$

The inertia weight coefficient w is a control parameter that is used to control the impact of the previous velocities on the current velocity. Hence, it influences the trade-off between the global and local exploration abilities of the particles. At the initial stage of the search process, large inertia weight is recommended to enhance the global exploration; while at its last stage, the inertia weight is reduced for better local exploration. As pointed out in Ref. [21], in order to prevent the particle from oscillating near the location of the global best fitness, a weight coefficient w is selected to decrease linearly: $w(t) = 0.9 - \frac{t}{N} \times 0.5$, where N means the maximum generation number and t is the iterative generation. However, for different problems, the proportional relation of particle velocities at every generation t is not the same, and the linear decreasing regulation of inertia weight coefficient is only effective for some optimal problems. For this limitation in solving different problems, Shi et al. [22] presented a fuzzy adaptive PSO to regulate the inertia weight coefficient dynamically.

2.2.2. Constriction factor approach of PSO

To ensure convergence of PSO algorithm, Clerc [23] presented a new PSO, which introduced a constrained factor α into Eq. (1) as follows:

$$\mathbf{V}_i(t+1) = \alpha \cdot \left\{\mathbf{V}_i(t) + c_1 \cdot r_1 \cdot \left[\mathbf{P}_i(t) - \mathbf{X}_i(t)\right] + c_2 \cdot r_2 \cdot \left[\mathbf{P}_g(t) - \mathbf{X}_i(t)\right]\right\} \tag{4}$$

where $\alpha = \frac{2}{|2-l-\sqrt{l^2-4l}|}$ with $l = c_1 + c_2$, $l > 4$. Both in simple PSO and Constriction Factor Approach (CFA) of PSO, maximum and minimum velocities are set to a priori values to avoid the infeasible combinations. In simple PSO, these values are kept constant. However, in CFA-PSO, the velocity is modified by a factor known as constriction factor α which is calculated from setting parameters c_1 and c_2. Once α is properly determined, the velocities can be maintained in a constant interval without exceeding the set velocities. Tests on different kinds

of functions demonstrate that incorporation of Clerc's constriction factor into PSO can result in a significant improvement of convergence [23]. Besides, this modified PSO can search different regions efficiently by avoiding premature convergence, and generate higher-quality solution than standard PSO on some studied problems [24].

2.2.3. Canonical PSO (CPSO)

Based on the comprehensive experimental research on the parameters of PSO, Carlisle and Dozier [25] presented the Canonical PSO with the parameters setting as follows:

$$\mathbf{V}_i(t+1) = \begin{cases} \alpha \cdot \{\mathbf{V}_i(t) + c_1 \cdot r_1 \cdot [\mathbf{P}_i(t) - \mathbf{X}_i(t)] \\ \quad + c_2 \cdot r_2 \cdot [\mathbf{P}_g(t) - \mathbf{X}_i(t)]\}, \\ \quad \mathbf{X}_{\min} < \mathbf{X}_i(t) < \mathbf{X}_{\max} \\ 0, \quad \text{others} \end{cases} \tag{5}$$

$$\mathbf{X}_i(t+1) = \begin{cases} \mathbf{X}_i(t) + \mathbf{V}_i(t+1), & \mathbf{X}_{\min} < \mathbf{X}_i(t) < \mathbf{X}_{\max} \\ \mathbf{X}_{\max}, & \mathbf{X}_i(t) + \mathbf{V}_i(t+1) > \mathbf{X}_{\max} \\ \mathbf{X}_{\min}, & \mathbf{X}_i(t) + \mathbf{V}_i(t+1) < \mathbf{X}_{\min} \end{cases} \tag{6}$$

The optimal parameter settings are: $c_1 = 2.8$, $c_2 = 1.3$, $M = 30$, the combination of all these parameters is called in this paper 'the classical parameters'.

2.2.4. Other Variants of PSO

In addition to the basic variants of PSO above, various other variant models of PSO have been developed in recent years. Based on the ecological niche ideology, Suganthan [26] presented a Local Best model with the neighborhood operator and Kennedy [27] studied different neighbourhood topology structures such as 'Ring Topology', 'Wheel Topology' and their random form topology. Based on the analysis of convergence character of PSO, Van Den Bergh [28] presented a modified PSO named as Guaranteed Convergence PSO (GCPSO) and discussed its strong local-convergence ability with weak global-convergence ability [29]. More recently, Van Den Bergh et al. [30] has presented a cooperative particle swarm optimizer (CPSO) to improve the performance of the original PSO, which is achieved by using multiple swarms to optimize different components of the solution vector cooperatively. Based on the genetic ideology, Angeline [31,32] presented the modified hybrid PSO by introducing the competitive selection mechanism and the cross mechanism of GA, respectively. Shi et al. [33] have presented a combined PSO-GA-based hybrid algorithm (PGHA) to solve the optimization problems, which executes the GA and PSO simultaneously to synthesize the merits of both PSO and GA.

2.3. SPSO algorithm

In present paper, we proposed a novel SPSO based on the analysis of convergence character of PSO. Considering the convergence research of PSO, Ozcan et al. [34] have proved that the PSO can guarantee convergence, but cannot guarantee global optimum. Solis and Wets [35] presented the necessary conditions of global convergence of random search techniques. According to these conditions, Van den Bergh [36] studied the global convergence and local convergence of basic PSO and GCPSO, respectively. As he pointed out, the basic PSO could not guarantee the global or local convergence [36]. However, in present paper, we proposed a novel SPSO algorithm which can guarantee the convergence of the global optimum solution with probability one.

In the standard PSO, when the current position of particle i is the global best position of particle swarm $\mathbf{X}_i(t) = \mathbf{P}_i(t) = \mathbf{P}_g(t)$, the second and third term in Eq. (3) will be zero, and Eq. (3) is transformed as: $\mathbf{V}_i(t+1) = w \cdot \mathbf{V}_i(t)$. In this equation, for there is only one term which regulates historic velocity, the ith particle will fly along one direction until it finds a better position or gets to the boundary. However, for the whole searching domain, the probability of finding a better solution along a straight-line is almost zero, i.e., the searching efficiency is quite low. In addition, if $w < 1$, then $\mathbf{V}_i(t+1) < \mathbf{V}_i(t)$. Under this condition, a fixed number *Num* must exist that when $t > Num$, the current global best position $\mathbf{P}_g$ of the swarm does not vary, and consequently, all components of $\mathbf{V}_i(t)$ will be smaller than ε (ε is a given error), i.e., the particle will stop evolution. Even if a better solution exists in this direction, the particle swarm may stop evolution before finding this position and fall into premature convergence. This is the reason why the standard PSO may fall into local optimum solution.

To solve the problem of premature convergence of standard PSO, we introduce the SPSO algorithm. In the standard PSO described by Eqs. (2) and (3), when $w = 0$, the velocity of ith particle only depends on the current position $\mathbf{X}_i(t)$, the historic best position $\mathbf{P}_i(t)$ and $\mathbf{P}_g(t)$, the velocity has no memory itself. The particle at the global best position will stop evolution, other particles will fly to the weighted center between their local best position and the global position, i.e., the particle swarm will concentrate to the global best position $\mathbf{P}_g$ which is more like a local algorithm. When $w \neq 0$, the particles have the ability to stretch the searching domain. This ability is enhanced with the increasing w value. Based on the analysis above, when $w = 0$, substituting Eq. (3) into Eq. (2), the following equation can be obtained:

$$\mathbf{X}_i(t+1) = \mathbf{X}_i(t) + c_1 \cdot r_1 \cdot \big[\mathbf{P}_i(t) - \mathbf{X}_i(t)\big] + c_2 \cdot r_2 \cdot \big[\mathbf{P}_g(t) - \mathbf{X}_i(t)\big] \tag{7}$$

Compared with the basic PSO, the evolutionary function described by Eq. (7) decrease the global searching ability but increase the local searching ability. When $\mathbf{X}_i(t) = \mathbf{P}_i = \mathbf{P}_g$, the particle will stop evolution. In order to improve the global searching ability of Eq. (7), $\mathbf{P}_g$ is maintained to be the historic best position, and random particle j with the position $\mathbf{X}_j(t+1)$ is generated randomly in the searching domain, while other particles $\mathbf{X}_i(t)$ $(i \neq j)$ in the population are updated by Eq. (7). In this way, the following updating procedure is obtained:

$$\mathbf{P}_j(t+1) = \mathbf{X}_j(t+1)$$

$$\mathbf{P}_i(t+1) = \begin{Bmatrix} \mathbf{P}_i(t+1), & F[\mathbf{P}_i(t+1)] < F[\mathbf{X}_i(t+1)] \\ \mathbf{X}_i(t+1), & F[\mathbf{P}_i(t+1)] \geqslant F[\mathbf{X}_i(t+1)] \end{Bmatrix}$$

$$\mathbf{P}'_g(t+1) = \arg\min\{F[\mathbf{P}_i(t+1)] \mid i = 1, \ldots, M\}$$
$$\mathbf{P}_g(t+1) = \arg\min\{F[\mathbf{P}'_g(t+1)], F[\mathbf{P}_g(t+1)]\} \quad (8)$$

If $\mathbf{P}_g = \mathbf{P}_j$, the random particle j locates at the best position and the new random particle will be searched repeatedly in the searching domain; and if $\mathbf{P}_g \neq \mathbf{P}_j$ and the global best position $\mathbf{P}_g$ is not updated, all the particles are updated by Eq. (7); if $\mathbf{P}_g \neq \mathbf{P}_j$ and the global best position $\mathbf{P}_g$ is updated, a particle k ($k \neq j$) with $\mathbf{X}_k(t+1) = \mathbf{P}_k = \mathbf{P}_g$ must exist, then particle k stops evolving and a new random particle is generated repeatedly in the searching domain. Thus, at certain generation in the evolutionary procedure, there is at least one particle j satisfying $\mathbf{X}_j(t+1) = \mathbf{P}_j = \mathbf{P}_g$. It means that at least one particle is generated in the searching domain randomly to improve the global searching ability of PSO algorithm. The flowchart of the SPSO algorithm is shown in Fig. 3.

Here, the convergence procedure of SPSO is presented briefly as follows. By defining $\varphi_1 = c_1 r_1$, $\varphi_2 = c_2 r_2$ and $\varphi = \varphi_1 + \varphi_2$, Eq. (7) could be transformed as:

$$\mathbf{X}_i(t+1) = (1-\varphi)\mathbf{X}_i(t) + \varphi_1 \cdot \mathbf{P}_i(t) + \varphi_2 \cdot \mathbf{P}_g(t) \quad (9)$$

If $\mathbf{P}_i$ and $\mathbf{P}_g$ are assumed to be constant, Eq. (9) becomes a simple linear difference equation. When $\mathbf{X}_i(0) = x_{i0}$, the solution of Eq. (9) is obtained:

$$\mathbf{X}_i(t) = k + (x_{i0} - k) \cdot (1-\varphi)^t \quad (10)$$

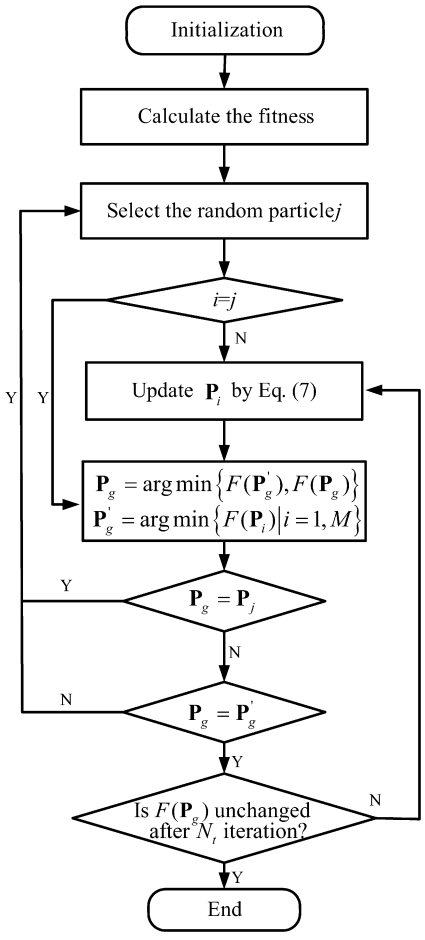

Fig. 3. The flowchart of the SPSO algorithm.

where $k = \frac{\varphi_1 \mathbf{P}_i + \varphi_2 \mathbf{P}_g}{\varphi}$. It should be noted that Eq. (10) is obtained based on the hypothesis of the fixed $\mathbf{P}_i$ and $\mathbf{P}_g$. However, during the evolution procedure of SPSO, the $\mathbf{P}_i$ and $\mathbf{P}_g$ may be updated at any generation. If $\mathbf{P}_i$ or $\mathbf{P}_g$ is updated, the value of k and x_{i0} will be reset. From Eq. (10), it can be seen that when $|1-\varphi| < 1$, then

$$\lim_{t\to\infty} \mathbf{X}_i(t) = k = \frac{\varphi_1 \mathbf{P}_i + \varphi_2 \mathbf{P}_g}{\varphi} \quad (11)$$

and

$$\mathbf{X}_i(t+1) = \mathbf{X}_i(t) - (\varphi_1 + \varphi_2)\mathbf{X}_i(t) + \varphi_1 \mathbf{P}_i + \varphi_2 \mathbf{P}_g \quad (12)$$

When $t \to \infty$,

$$\lim_{t\to\infty} \mathbf{X}_i(t+1) = \lim_{t\to\infty} \mathbf{X}_i(t) \quad (13)$$

then

$$-(\varphi_1 + \varphi_2) \lim_{t\to\infty} \mathbf{X}_i(t) + \varphi_1 \mathbf{P}_i + \varphi_2 \mathbf{P}_g = 0 \quad (14)$$

For φ_1 and φ_2 are random variables, could Eq. (14) be satisfied only when $\lim_{t\to\infty} \mathbf{X}_i(t) = \mathbf{P}_i = \mathbf{P}_g$. Thus, when $|1-\varphi| < 1$ the evaluation equation described by Eq. (9) converges linearly. Meanwhile, according to $|1-\varphi| < 1$, we can get $0 < c_1 + c_2 < 2$ which is the necessary condition for the convergence of SPSO. The detailed theoretical certification of the global convergence with probability one of SPSO is reported in Ref. [37] by Zeng et al. based on the necessary conditions of global convergence of PSO presented by Solis and Wets [35]. In a word, compared with standard PSO, SPSO eliminates the historical velocity term which makes the particle lose velocity memory to decrease the global searching ability. But it guarantees at every generation one particle stops evolution for locating at the best position. The basic idea of SPSO is the usage of the stopping evolution particle to improve the global searching ability. For the global convergence, SPSO could guarantee but PSO could not. When the generation $t \to \infty$, SPSO could guarantee the convergence of the global optimum solution with probability one.

3. Computation procedures of PSO-based approaches

The implementation of the PSO-based approach for solving the inverse radiative problem can be carried out according to the following routine.

Step 1. Input system data, and initialize a particle swarm. Input system configuration, control parameters such as lower and upper bounds of estimated radiative parameters, the number of dimensions n of each particle. Randomly generate an initial swarm of particles with random positions and velocities on n-dimensions in the solution space. Set the index of iteration $t = 0$.

Step 2. Calculate the fitness value. For each particle, first calculate the initial fitness by substituting the position of each particle into the forward radiative problems. The fitness value is set equal to the calculated value of objective function with argument of each particle position.

Step 3. For each particle, compare its fitness value with a priori best $\mathbf{P}_i$. If the fitness value is lower than $\mathbf{P}_i$, set this value as the current $\mathbf{P}_i$, and record the corresponding particle position.

Step 4. Choose the particle associated with the best $\mathbf{P}_i$ of all particles, and set the value of this $\mathbf{P}_i$ as the current global best $\mathbf{P}_g$.

Step 5. For each particle, calculate the new velocity using Eq. (1), and then update the particle position using Eq. (2).

Step 6. Check the stop criterion. If the maximum number of generation set a priori is reached or the non-improvement of the best solution after a given number of iterations N_t is obtained, go to Step 7; otherwise, set iteration index $t = t + 1$, and loop to Step 2.

Step 7. Print out the optimal solution (the best position and the corresponding fitness value) to the radiative inverse problem.

For SPSO, the main change of computational procedure is introducing a randomly-selected particle into the population before each iterative loop as shown in Fig. 3.

4. Test results of PSO and SPSO

To test the performance of the proposed SPSO, three famous benchmark optimization functions are used, which are described in Table 1. The standard PSO uses a linearly varying inertia weight over the generations, varying from 0.9 at the beginning of the search to 0.4 at the end. The particle swarm is 50, and $c_1 = c_2 = 2.0$. The c_1 and c_2 of SPSO are set to 1.0. The global minimum of these three functions are all zero, the criterion of convergence is defined as: the iteration accuracy 10^{-10} is achieved or the iteration is more than the fixed total number of function evaluation. Table 2 lists the average best function value and the standard deviation of 50 independent runs. From Table 2, it can be seen that the results of SPSO are much closer to the theoretical optima, and SPSO is superior to PSO in term of searching quality and derivation of the results. So it is concluded that SPSO is more effective and it is more robust on initial conditions. From Figs. 4–6, it can be seen that the varying curves of average fitness values using SPSO descend much faster than those using PSO, and the objective fitness values descent to lower level by using SPSO than using PSO. So, it is concluded that SPSO is more efficient than PSO, and the final searching quality of SPSO is better than PSO.

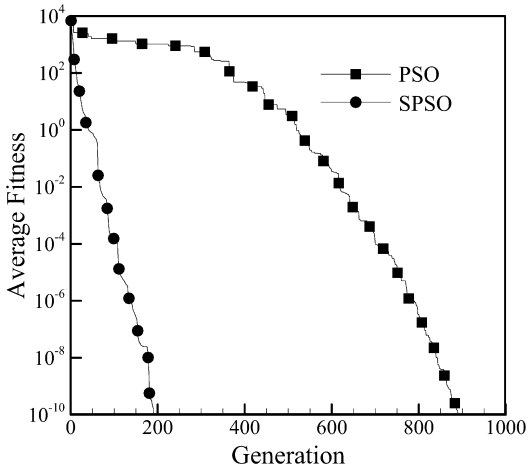

Fig. 4. Comparison of average best fitness of PSO and SPSO for Sphere function.

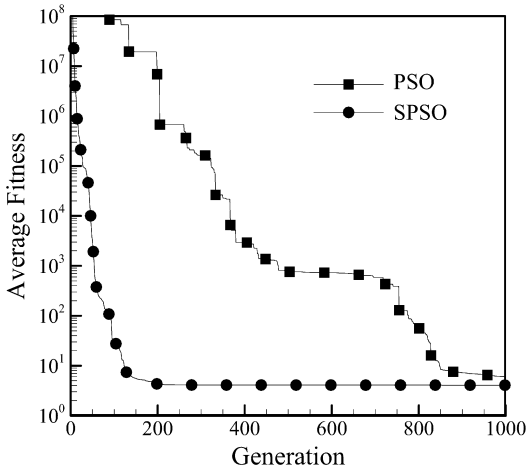

Fig. 5. Comparison of average best fitness of PSO and SPSO for Rosenbrock function.

Table 1
Details of test functions

Function	Expression	Dimension	Space	$\mathbf{V}_{\max}$
Sphere	$f_1 = \sum_{i=1}^{n} x_i^2$	10	$[-100, 100]^n$	100
Rosenbrock	$f_2 = \sum_{i=1}^{n} [100(x_{i+1} - x_i^2)^2 + (x_i - 1)^2]$	10	$[-100, 100]^n$	100
Griewank	$f_3 = \frac{1}{4000} \sum_{i=1}^{n} x_i^2 - \prod_{i=1}^{n} \cos(\frac{x_i}{i^{1/2}}) + 1$	10	$[-600, 600]^n$	600

Table 2
Fixed-iteration results of 50 runs

Function	PSO	SPSO	Iteration
Sphere	$2.588 \times 10^{-12} \pm 8.985 \times 10^{-13}$	$2.774 \times 10^{-27} \pm 3.522 \times 10^{-27}$	500
Rosenbrock	$18.910 \pm 4.018 \times 10^{1}$	$7.103 \pm 1.103 \times 10^{1}$	3000
Griewank	$0.124 \pm 7.304 \times 10^{-2}$	$0.077 \pm 1.149 \times 10^{-2}$	500

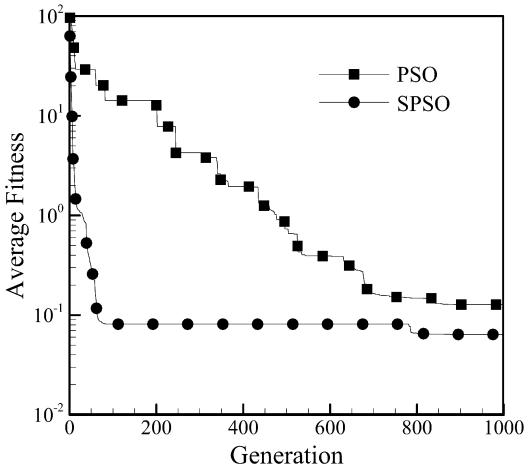

Fig. 6. Comparison of average best fitness of PSO and SPSO for Griewank function.

5. Inverse radiative simulation by PSO and SPSO

To demonstrate the validity of the proposed PSO and SPSO in inverse radiative analysis, three different test cases are considered in present study. Firstly, the accuracy and efficiency comparison of PSO and SPSO on the estimation of source term is considered. Secondly, the extinction coefficient and scattering coefficient are estimated by SPSO from the reflectance and transmittance for 1D slab with normal incidence. Finally, the non-uniform distribution of absorbing coefficients in non-scattering media is estimated as well to verify the feasibility of SPSO on retrieving the discrete parameters. The proposed PSO-based algorithm in each case was implemented using FORTRAN code and the developed program was executed on an AMD 2500+ PC. In our implementation, the parameters of standard PSO are set as follows: both coefficients c_1 and c_2 were 2.0 as those in Ref. [38]; the inertia weight decreased linearly from 0.9 down to 0.4 throughout the run for standard PSO. The search will be terminated if the total number of iterations reaches 10, 000 or the non-improvement of the best solution after a given number of iterations $N_t = 1000$ is obtained. To demonstrate the effects of measurement errors on the inversed parameters, random standard deviation are added to the exact parameters computed from the direct solution, the following relations have been used in present inverse analysis:

$$Y_{\text{mea}} = Y_{\text{exact}} + \sigma\varsigma \tag{15}$$

Here, ς is a normal distribution random variable with zero mean and unit standard deviation. The standard deviations of measured radiative intensities at the boundaries, σ for a $\gamma\%$ measured error at 99% confidence, are determined as

$$\sigma = \frac{Y_{\text{exact}} \times \gamma\%}{2.576} \tag{16}$$

For the sake of comparison, relative error ε_{rel} is defined as follows

$$\varepsilon_{\text{rel}} = 100 \times \frac{Y_{\text{est}} - Y_{\text{exact}}}{Y_{\text{exact}}} \tag{17}$$

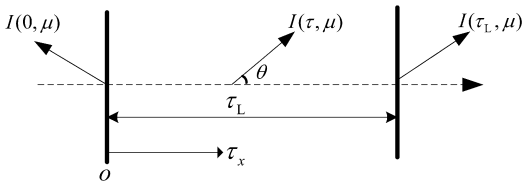

Fig. 7. Schematic of the physical system and coordinates of 1D slab.

Case 1: Inverse estimation of the source term with PSO and SPSO

To examine the accuracy and computational efficiency of the PSO-based algorithm presented in this paper, a relatively simple source term inverse problem for 1D plane-parallel gray media is presented. The schematic of the 1D slab is depicted in Fig. 7. The direct analytical solutions for this problem are developed in Ref. [39]:

$$I^+(\tau,\mu) = I_{\text{b1}} e^{-\tau/\mu} + \frac{1}{\mu}\int_0^\tau S(\tau') e^{-(\tau-\tau')/\mu}\,\mathrm{d}\tau' \quad 0 < \mu < 1 \tag{18}$$

$$I^-(\tau,\mu) = I_{\text{b2}} e^{(\tau_{\text{L}}-\tau)/\mu} - \frac{1}{\mu}\int_\tau^{\tau_{\text{L}}} S(\tau') e^{(\tau'-\tau)/\mu}\,\mathrm{d}\tau' \quad -1 < \mu < 0 \tag{19}$$

With boundary conditions $I_{\text{b1}} = I_{\text{b2}} = 0$, where I is radiative intensity, τ is the optical thickness and $\mu = \cos\theta$ is the directional cosine. We assume that the source term $S(\tau)$ is represented by a polynomial in the optical thickness variable τ as

$$S(\tau) = \sum_{i=1}^{n} a_i \tau^{i-1} \tag{20}$$

For inverse calculation, the coefficient array $\mathbf{a} = [a_1, a_2, a_3]^{\text{T}}$ of internal source term is retrieved by utilizing the measured exit directional radiation intensities at the slab boundary (10 measurement points over the directional angle interval $0 \leqslant \theta \leqslant \pi$ are used in present paper). In this case, the exact coefficient of source term distribution is assumed as $\mathbf{a} = [a_1, a_2, a_3]^{\text{T}} = [1, 5, -5]^{\text{T}}$.The objective function for minimization is defined as follows:

$$F(\mathbf{a}) = \left\|\mathbf{I}_{\text{mea}}(\mathbf{a},\mu,\tau_0) - \mathbf{I}_{\text{est}}(\mathbf{a},\mu,\tau_0)\right\|_{\text{L}_2} + \left\|\mathbf{I}_{\text{mea}}(\mathbf{a},\mu,\tau_{\text{L}}) - \mathbf{I}_{\text{est}}(\mathbf{a},\mu,\tau_{\text{L}})\right\|_{\text{L}_2} \tag{21}$$

where

$$\begin{cases} \tau = \tau_0, & -1 \leqslant \mu \leqslant 0 \\ \tau = \tau_{\text{L}}, & 0 \leqslant \mu \leqslant 1 \end{cases}$$

$F(\mathbf{a})$ is the residual of boundary directional intensity.

It should be noticed that the range of $[x_{\min}, x_{\max}]$ is determined according to the real physics of source term which must be positive. As the individual particle is selected randomly, there exists a possibility of obtaining a particle with negative

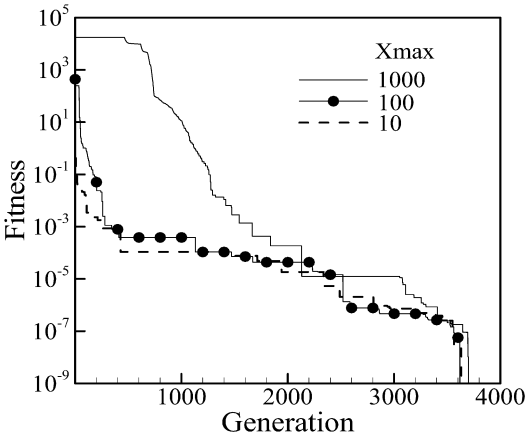

Fig. 8. Comparison of fitness function with different $\mathbf{X}_{\max}$ with fixed $\mathbf{V}_{\max}$.

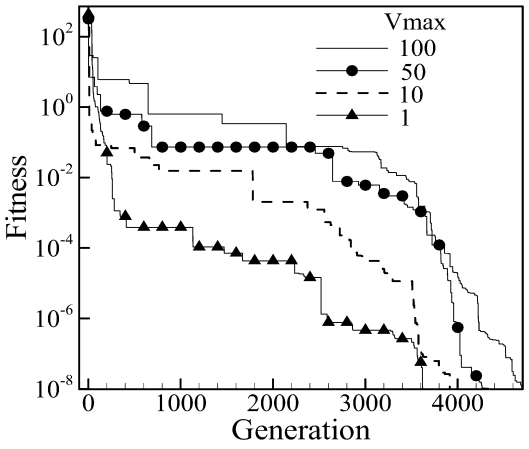

Fig. 9. Comparison of fitness function with different $\mathbf{V}_{\max}$ with fixed $\mathbf{X}_{\max}$.

position $\mathbf{X}_i$ which is not physically meaningful. For this reason, if the source term is selected to be negative, a threshold fitness function of source term is defined as follow:

$$F(\mathbf{X}_i) = \begin{cases} 10^5, & S(\mathbf{X}_i) \leqslant 0 \\ \text{Updated by PSO}, & S(\mathbf{X}_i) > 0 \end{cases} \tag{22}$$

Using this threshold fitness function, the infeasible solution with negative source could be eliminated in the procedure of PSO-based algorithm. This technique is used in all the test cases throughout this paper.

The influence of different range $[x_{\min}, x_{\max}]$ on the fitness function of standard PSO is examined firstly. For the sake of comparison, all the components of array $\mathbf{X}_{\min}$ and $\mathbf{X}_{\max}$ are set as the same value and the ranges of $[x_{\min}, x_{\max}]$ are set as $[-10, 10]$, $[-100, 100]$, $[-1000, 1000]$ with fixed $v_{\max} = 1$, respectively. As shown in Fig. 8, the fitness objective function of standard PSO converges more quickly with smaller $x_{\max}$ value. Meanwhile, the influence of different $v_{\max}$ on the best fitness function of PSO is studied as well. Assuming the range of $[x_{\min}, x_{\max}]$ is set as $[-100, 100]$, different $v_{\max}(1, 10, 50, 100)$ is selected. As shown in Fig. 9, the fitness objective function of standard PSO convergences faster with decreasing $v_{\max}$ value. In Case 1, the range of $[x_{\min}, x_{\max}]$ is set as $[-100, 100]$, and the $v_{\max}$ is set as 1.

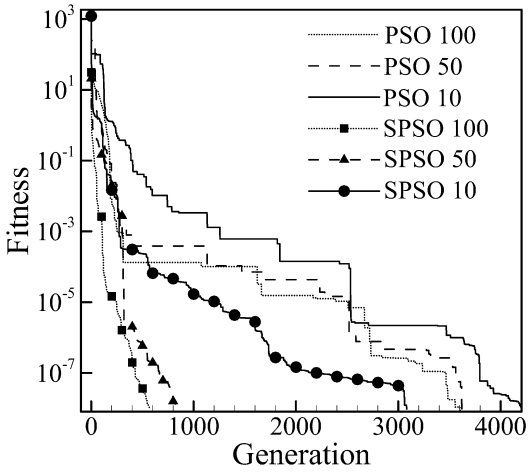

Fig. 10. Comparison of best fitness function of PSO and SPSO for different swarm size.

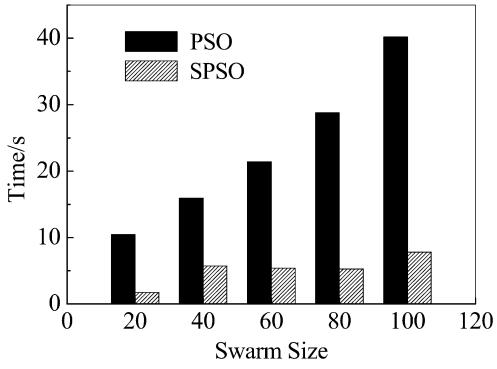

Fig. 11. Comparison of computation time of PSO and SPSO for different swarm size.

Table 3
Parameters setting of PSO and SPSO algorithm

Parameters	PSO	SPSO
$v_{\max}$	100	100
$[x_{\min}, x_{\max}]$	$[-100, 100]$	$[-100, 100]$
Swarm Size: M	[10, 50, 100]	[10, 50, 100]
Maximum Swarm: N	10 000	10 000
$c_1 \& c_2$	2.0	1.0

Without measurement errors, the performance of standard PSO is compared with SPSO for three different swarm sizes (or population sizes). A summary of the parameter settings for PSO and SPSO algorithm are shown in Table 3. As shown in Fig. 10, the best fitness objective function of SPSO algorithm converges much faster than standard PSO with same swarm size. With the swarm size increasing, both PSO and SPSO algorithm show more quickly convergent. As shown in Fig. 11, the SPSO is less time-consuming than PSO of the same swarm size. All the results show that SPSO is superior to the standard PSO in both the speed of convergence and the efficiency of computation. The effect of measured error on the accuracy by PSO and SPSO is examined for various standard deviations with swarm size $M = 50$ (In the sequel we employ $M = 50$, if not specified otherwise). The estimated results of PSO and SPSO are almost

Table 4
Inverse results with different measure errors using SPSO

Inverse parameter	True value	$\gamma=0$		$\gamma=1$		$\gamma=3$		$\gamma=5$	
		SPSO	ε_{rel} %	SPSO	ε_{rel} %	SPSO	ε_{rel} %	SPSO	ε_{rel} %
κ_e	1.0	1.0000	0.000	0.9909	0.91	0.9730	2.7	0.9554	4.46
κ_s	0.5	0.5000	0.000	0.5001	0.02	0.4998	0.04	0.4996	0.08
Inverse parameter	True value	$\gamma=0$		$\gamma=1$		$\gamma=3$		$\gamma=5$	
		SPSO	ε_{rel} %	SPSO	ε_{rel} %	SPSO	ε_{rel} %	SPSO	ε_{rel} %
κ_e	3.0	3.0000	0.000	2.9940	0.20	2.9822	0.59	2.9708	0.97
κ_s	1.5	1.5000	0.000	1.5066	0.44	1.5197	1.31	1.5329	2.19
Inverse parameter	True value	$\gamma=0$		$\gamma=1$		$\gamma=3$		$\gamma=5$	
		SPSO	ε_{rel} %	SPSO	ε_{rel} %	SPSO	ε_{rel} %	SPSO	ε_{rel} %
κ_e	5.0	5.0000	0.0000	4.9971	0.06	4.9916	0.17	4.9866	0.27
κ_s	2.5	2.5000	0.0000	2.5145	0.58	2.5432	1.73	2.5721	2.88
Inverse parameter	True value	$\gamma=0$		$\gamma=1$		$\gamma=3$		$\gamma=5$	
		SPSO	ε_{rel} %	SPSO	ε_{rel} %	SPSO	ε_{rel} %	SPSO	ε_{rel} %
κ_e	10.0	10.0002	0.002	10.0054	0.054	10.0167	0.167	10.0290	0.29
κ_s	5.0	5.0000	0.000	5.032	0.64	5.1035	2.07	5.1720	3.44

the same in fourth decimal point and the average relative error becomes negligible by PSO and SPSO without measurement errors. The measured error of $\gamma = 5\%$ corresponds to a possible maximum relative estimated error of 8.056%.

Case 2: Inverse estimation of the extinction coefficient and scattering coefficient with SPSO

Consider a normal incident radiation at the left boundary of absorbing, scattering and non-emitting slab, the equation of radiative transfer and the boundary conditions can be written as [40]:

$$\mu\frac{\partial I(\tau,\mu)}{\partial\tau} = -I(\tau,\mu) + \frac{\omega}{2}\int_{-1}^{1} I(\tau,\mu')\Phi(\mu,\mu')\,\mathrm{d}\mu' + \frac{\omega}{4\pi}q\Phi(\mu,1)e^{-\tau} \tag{23a}$$

$$I(0,\mu) = 0, \quad \mu \geqslant 0 \tag{23b}$$

$$I(\tau_{\text{L}},\mu) = 0, \quad \mu < 0 \tag{23c}$$

In this case, the reflectance ρ_R and transmittance ρ_T can be expressed as

$$\rho_R = -\frac{2\pi}{q}\int_{-1}^{0} I(0,\mu)\mu\,\mathrm{d}\mu \tag{24}$$

$$\rho_T = e^{-\tau_{\text{L}}} + \frac{2\pi}{q}\int_{0}^{1} I(\tau_{\text{L}},\mu)\mu\,\mathrm{d}\mu \tag{25}$$

The scattering phase function Φ of media is assumed to be linear anisotropic, given as $\Phi(\mathbf{s}^m, \mathbf{s}^{m'}) = 1 + g(\mathbf{s}^m \cdot \mathbf{s}^{m'})$, where g is the scattering asymmetry parameter. q is the normal incident radiation and L is the thickness of 1D slab. The parameters of this case are set as: $L = 1.0$ m, $g = 1$ and $q = 2\pi$ W m^{-2}. In the inverse analysis, the measured reflectance ρ_R and transmittance ρ_T data (obtained by forward calculation) is employed as input, and the extinction coefficient κ_e and scattering coefficient κ_s are estimated by minimizing the objective function that is the square deviation between the calculated and measured reflectance and transmittance.

$$F(\kappa_e,\kappa_s) = \left\|\rho_{R,\text{mea}}(\kappa_e,\kappa_s) - \rho_{R,\text{est}}(\kappa_e,\kappa_s)\right\|_{\text{L}_2} + \left\|\rho_{T,\text{mea}}(\kappa_e,\kappa_s) - \rho_{T,\text{est}}(\kappa_e,\kappa_s)\right\|_{\text{L}_2} \tag{26}$$

In the following analysis, the level symmetric hybrid (LSH) quadrature of DOM S_8 is used [41]. As presented in Ref. [42], the reflectance and transmittance is sensitive to variation of the extinction coefficient and scattering coefficient. Thus, the extinction coefficient and scattering coefficient could be retrieved from the measured reflectance and transmittance, which is much more important for the light reflectance and transmittance experiment to obtain the radiative properties of the medium.

Here, the results with different extinction coefficient and scattering coefficient estimated by using SPSO are shown in Table 4. From Table 4, it can be seen that with no measurement errors, the agreement between the estimated and the exact values of the radiative parameters is excellent. Simulated experimental data containing measurement errors of $\gamma\%$ ranges from 0 to 5% are used to estimate the retrieved results of extinction coefficient and scattering coefficient. Clearly, with the measured error $\gamma\%$ increasing, the accuracy of the estimation decreases. Meanwhile, the influence of optical thickness on the accuracy of the estimation was also examined in Table 4. As the optical thickness increases, the accuracy of the estimation becomes more sensitive to the measurement errors. In case of $\gamma\% = 5\%$, the maximum relative error $\varepsilon_{\text{rel}}\%$ of κ_s is up to about 3.44%; the maximum relative error $\varepsilon_{\text{rel}}\%$ of κ_e is less than 4.46%. With the optical thickness increasing, the relative error of κ_s increases gradually, while the relative error of κ_e decreases. It should be noted that when the optical thickness is larger than 10, κ_e and κ_s could not be estimated reasonably. The reason is that as the optical thickness increases, the measurement signal of reflectance

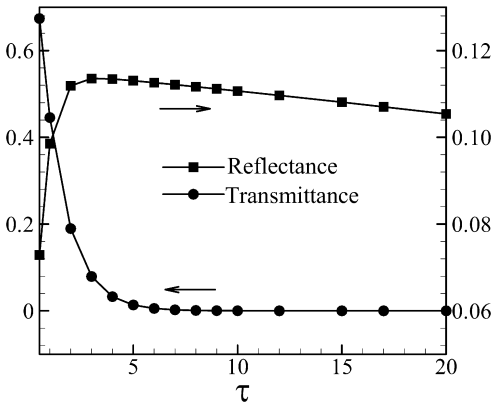

Fig. 12. The variation of Reflectance and Transmittance with different optical thickness.

ρ_R approaches to a constant ($\rho_R \to 0.0105$ in this case) and the transmittance ρ_T data approaches to a much smaller number (about $< 10^{-4}$), as indicated in Fig. 12. Thus, it is a necessary condition that the optical thickness could not be too large ($\tau \leqslant 10$) for the radiative inverse analysis in Case 2.

Case 3: Inverse estimation of the non-uniform absorbing coefficient using SPSO

In order to test the feasibility of SPSO in calculating the inverse radiation problem with an array of discrete parameters, we consider the radiative transfer in a 1D slab filled with non-scattering gray gas with spatially varying absorption coefficients along x-axis. The function of absorption coefficients are assumed as:

$$\mu \frac{\partial I(x,\mu)}{\partial x} = -\kappa_a(x) \cdot I(x,\mu) + \kappa_e(x) \cdot I_b(x) \tag{27a}$$

with boundary conditions

$$I(0,\mu) = \varepsilon_1 \frac{\sigma T_0^4}{\pi}, \quad \mu > 0$$
$$I(\mathrm{L},\mu) = \varepsilon_2 \frac{\sigma T_L^4}{\pi}, \quad \mu < 0 \tag{27b}$$

where ε_1 and ε_2 are the emissivities of the two boundaries, respectively, κ_a is the absorption coefficient, κ_e is the extinction coefficient which is equal to κ_a in this case. A control volume form of the discrete ordinates equations can be obtained by integrating Eq. (27) over the cell volume, from which we have

$$\int_{\Delta x} \mu \frac{\partial I(x,\mu)}{\partial x}\,\mathrm{d}x = \int_{\Delta x} \left[-\kappa_a(x) \cdot I(x,\mu) + \kappa_e(x) \cdot I_b(x)\right]\mathrm{d}x \tag{28a}$$

$$\mu(I_u - I_d) = -\kappa_a I_p \Delta x + \kappa_e I_{b,p} \Delta x \tag{28b}$$

where Δx is the thickness of gas media volume element. The nodal radiation intensity I_p can be expressed in terms of radiative intensities at the upstream and the downstream boundaries of control volume, I_u and I_d, by using the following differencing form:

$$I_p = I_u(1-f) + I_d f \tag{29}$$

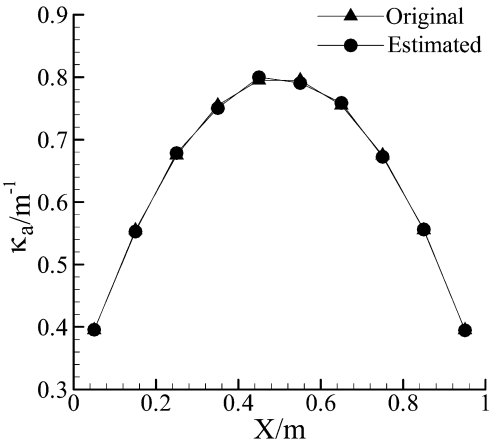

Fig. 13. The original and estimated distribution of absorption coefficients with $\gamma = 0$.

where f is the differencing factor. The diamond scheme with $f = 0.5$ is used in this paper. The nodal radiative intensity I_p at the center of the control volume element can therefore be evaluated as

$$I_p = \frac{|\mu| I_d + \kappa_e f I_{b,p} \Delta x}{|\mu| + \kappa_a f \Delta x} \tag{30}$$

The solution of the discrete ordinates equations Eq. (27) of radiative transfer equation must be obtained iteratively. The detailed procedure of the solution can be seen in Ref. [39], and will not be repeated here.

In this case, the thickness of gas slab is set as L = 1.0 m, the boundaries are gray walls with temperature $T_0 = 1500$ K and $T_L = 1000$ K, $\varepsilon_1 = \varepsilon_2 = 0.8$. The absorption coefficient κ_a is assumed as follows:

$$\kappa_a(x) = -2(x/L - 0.5)^2 + 0.8\ (\mathrm{m}^{-1}) \tag{31}$$

For inverse calculation, ten spatially varying absorption coefficients κ_a are retrieved from the measurement radiative flux. The objective function for minimization is defined as follows:

$$F(\boldsymbol{\kappa}_a) = \left\| \mathbf{q}_{\mathrm{mea}}(\tau_x) - \mathbf{q}_{\mathrm{est}}(\tau_x) \right\|_{L_2}, \quad \tau_0 \leqslant \tau_x \leqslant \tau_L \tag{32}$$

where $\mathbf{q}$ is the array of radiative flux. The estimated results with no errors and effects of measurement errors on the accuracy of estimation are shown in Figs. 13 and 14, respectively. As shown in Fig. 13 without measurement errors, the results of non-uniform absorption coefficients are retrieved accurately. From Fig. 14, it can be seen that the non-uniform absorption coefficients of 1D slab could be estimated with reasonable accuracy by SPSO even with the noisy measurement flux. As expected, the accuracy of estimation deteriorates as the measurement error increases, and the maximum relative error with $\gamma\% = 5\%$ is smaller than 4%.

6. Conclusions

A novel PSO-based algorithm SPSO, which can guarantee the convergence of the global optimization solution with probability one, is adopted to estimate parameters of radiation system by minimizing an objective function, expressed

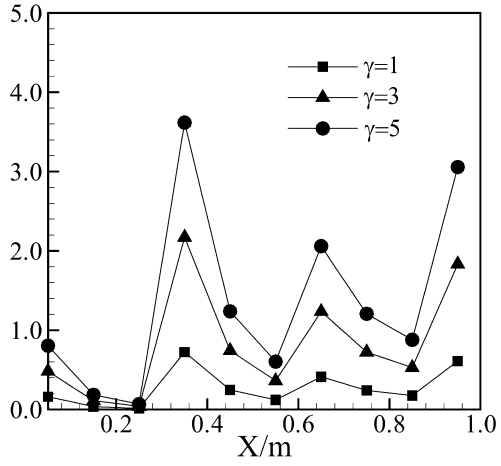

Fig. 14. The influence of measurement errors on the relative errors of estimated results.

by the sum of square errors between estimated and measured radiative intensity, the reflectance and transmittance, or the radiative flux. These inverse radiation analyses were carried out for the source term or the radiative properties, i.e., the extinction coefficient, scattering coefficient, and absorption coefficient, for an absorbing, emitting and scattering media in a 1D slab with diffusely emitting and reflecting opaque boundaries. In these cases, SPSO is proved to be superior to the standard PSO in both convergence speed and computation efficiency. Meanwhile, by using SPSO, these radiative parameters can be estimated accurately even with noisy data. In conclusion, the optimization algorithm SPSO is proved to be fast and robust, which has the potential to be implemented in the field of various inverse radiation problems. It is also suggested the PSO-based algorithms to be used when the traditional optimization methods fail, or are difficult to be applied to some inverse radiation problems. Further study will focus on the performance improvement of the PSO-based methodology as well as other applications of PSO in the multi-dimensional radiative inverse analysis in non-gray media.

Acknowledgements

The support of this work by National Natural Science Foundation of China (No. 50576019) and the key project of the National Natural Science Foundation of China (Grant. No.50336010) are gratefully acknowledged.

References

[1] N.J. McCormick, Methods for solving inverse problems for radiation transport—an update, Transport Theory Statist. Phys. 15 (1986) 759–772.
[2] N.J. McCormick, Inverse radiative transfer problems: A review, Nuclear Sci. Engrg. 112 (1992) 185–198.
[3] S. Subramaniam, M.P. Menguc, Solution of the inverse radiation problem for inhomogeneous and anisotropically scattering media using a Monte Carlo technique, Int. J. Heat Mass Transfer 34 (1991) 253–266.
[4] M.P. Menguc, S. Manickavasagam, Inverse radiation problem in axisymmetric cylindrical scattering media, J. Thermophys. Heat Transfer 7 (1993) 479–486.
[5] D.A. Ligon, T.W. Chen, J.B. Gillespie, Determination of aerosol parameters from light-scattering data using an inverse Monte Carlo technique, Appl. Optics 35 (1996) 4297–4303.
[6] A.J.S. Neto, M.N. Ozisik, An inverse problem of simultaneous estimation of radiation Phase function, albedo and optical thickness, J. Quant. Spectrosc. Radiat. Transfer 53 (1995) 397–409.
[7] L.B. Barichello, R.D.M. Garcia, C.E. Siewert, On inverse boundary-condition problems in radiative transfer, J. Quant. Spectrosc. Radiat. Transfer 57 (1997) 405–410.
[8] L.H. Liu, H.P. Tan, Z.H. He, Inverse radiation problem of source term in three-dimensional complicated geometric semitransparent media, Int. J. Therm. Sci. 40 (2001) 528–538.
[9] H.Y. Li, Inverse radiation problem in two-dimensional rectangular Media, J. Thermophys. Heat Transfer 11 (1997) 556–561.
[10] M.P. Menguc, S. Manickavasagam, Inverse radiation problem in axisymmetric cylindrical scattering media, J. Thermophys. Heat Transfer 7 (1993) 479–486.
[11] C. Elegbede, Structural reliability assessment based on particles swarm optimization, Structural Safety 27 (2005) 171–186.
[12] K.W. Kim, S.W. Baek, M.Y. Kim, H.S. Ryou, Estimation of emissivities in a two-dimensional irregular geometry by inverse radiation analysis using hybrid genetic algorithm, J. Quant. Spectrosc. Radiat. Transfer 87 (2004) 1–14.
[13] J. Kennedy, The particle swarm: social adaptation of knowledge, in: Proc. 1997 IEEE International Conference of Evolutionary Computation, ICEC'97, Indianapolis, IN, USA, 1997, pp. 303–308.
[14] M. Schoenauer, Z. Michalewicz, Evolutionary computation: An introduction, Control Cybern. 26 (1997) 307–338.
[15] R. Eberhart, J. Kennedy, A new optimizer using particle swarm theory, in: Proceedings of the 1995 Sixth International Symposium on Micro Machine and Human Science, 1995, pp. 39–43.
[16] J. Kennedy, R.C. Eberhart, Particle swarm optimization, in: Proc. IEEE Int'1. Conf. on Neural Networks, IV, IEEE Service Center, Piscataway, NJ, 1995, pp. 1942–1948.
[17] S. Kannan, S.M.R. Slochanal, P. Subbaraj, N.P. Padhy, Application of particle swarm optimization technique and its variants to generation expansion planning problem, Electric Power Syst. Res. 70 (2004) 203–210.
[18] P.Y. Yin, A discrete particle swarm algorithm for optimal polygonal approximation of digital curves, J. Visual Commun. Image Represent. 15 (2004) 241–260.
[19] A. Salman, I. Ahmad, S.A. Madani, Particle swarm optimization for task assignment problem, Microprocess. Microsyst. 26 (2002) 363–371.
[20] Y. Shi, R.C. Eberhart, A modified particle swarm optimizer, in: Proceedings of the IEEE International Conference on Evolutionary Computation, IEEE Press, Piscataway, NJ, 1998, pp. 69–73.
[21] Y. Shi, R.C. Eberhart, Empirical study of particle swarm optimization, in: Proceedings of the 1999 Congress on Evolutionary Computation, IEEE Service Center, Piscataway, NJ, 1998, pp. 1945–1950.
[22] Y. Shi, R.C. Eberhart, Fuzzy adaptive particle swarm optimization, in: Proc. Congress on Evolutionary Computation 2001, IEEE Service Center, Seoul, Korea, 2001.
[23] M. Clerc, The swarm and the Queen: Towards a deterministic and adaptive particle swarm optimization, Proc. CEC 1999 (1999) 1951–1957.
[24] Y. Shi, R.C. Eberhart, Comparing inertia weights and constriction factors in particle swarm, in: Proceedings of the 2000 Congress on Evolutionary Computation, 2000, pp. 84–88.
[25] A. Carlisle, G. Dozier, An off-the-self PSO, in: Proceedings of the Workshop on Particle Swarm Optimization, Indianapolis, in: Purdue School of Engineering and Technology, IUPUI, 2001.
[26] P.N. Suganthan, Particle swarm optimizer with neighbourhood operator, in: Proceedings of the 1999 Congress on Evolutionary Computation, IEEE Service Center, Piscataway, NJ, 1999, pp. 1958–1962.
[27] J. Kennedy, Small worlds and Mega-minds: Effects of neighbourhood topology on Particle Swarm performance, in: Proc. Congress on Evolutionary Computation, IEEE Service Center, Piscataway, NJ, 1999, pp. 1931–1938.

[28] F. Van den Bergh, A.P. Engelbrecht, A new locally convergent particle swarm optimizer, in: IEEE International Conference on Systems, Man, and Cybernetics, 2002.
[29] F. Van den Bergh, A.P. Engelbrecht, Particle swarm weight initialization in multi-layer perception artificial neural networks, in: Development and Practice of Artificial Intelligence Techniques, Durban, South Africa, 1999, pp. 41–45.
[30] F. Van den Bergh, A.P. Engelbrecht, A cooperative approach to particle swarm optimization, IEEE Trans. Evol. Comput. 8 (2004) 225–239.
[31] P.J. Angeline, Using selection to improve particle swarm optimization, in: IEEE International Conference on Evolutionary Computation, Anchorage, Alaska, USA, 1998, pp. 84–89.
[32] P.J. Angeline, Evolutionary optimization versus particle swarm optimization: Philosophy and performance differences, in: The Seventh Annual Conference on Evolutionary Programming, 1998.
[33] X.H. Shi, Y.C. Liang, H.P. Lee, C. Lu, L.M. Wang, An improved GA and a novel PSO-GA-based hybrid algorithm, Inform. Process. Lett. 93 (2005) 255–261.
[34] E. Ozcan, C. Mohan, Particle swarm optimization: Surfing the waves, in: Proc. of the Congress on Evolutionary Computation, IEEE Service Center, Piscataway, NJ, 1999, pp. 1939–1944.
[35] F. Solis, R. Wets, Minimization by random search techniques, Math. Operat. Res. 1 (1981) 19–30.
[36] F. Van den Bergh, An analysis of particle swarm optimizers, PhD dissertation, Pretoria, University of Pretoria, 2001.
[37] J.C. Zeng, Z.H. Cui, A guaranteed global particle swarm optimizer, J. Comput. Res. Development 41 (2004) 1333–1338 (in Chinese).
[38] J. Kennedy, Thinking a socail: Experiments with the adaptive culture model, J. Conflict Resolut. 42 (1998) 56–76.
[39] M.F. Modest, Radiative Heat Transfer, second ed., Academic Press, Burlington, 2003.
[40] M.Q. Brewster, Thermal Radiative Transfer and Properties, Wiley, New York, 1992.
[41] W.A. Fiveland, The selection of discrete ordinate quadrature sets for anisotropic scattering, Fundamentals of Radiation Heat Transfer, ASME HTD 160 (1991) 89–96.
[42] L.H. Liu, L.M. Ruan, Numerical approach for reflections and transmittance of finite plane-parallel absorbing and scattering medium subjected to normal and diffuse incidence, J. Quant. Spectrosc. Radiat. Transfer 75 (2002) 637–646.